Dressing of Diamond Grinding Wheels with Abrasive Water Jet for RB-SiC Surface Grinding

Zhenzhong Zhang [1, a], Chong Wang[1, b], Peng Yao[1, c*], Jun Wang[2, d], Chuanzhen Huang[1, e], Ke Zhang[3, f], Yue Liu[1, g]

[1] Key Laboratory of High Efficiency and Clean Mechanical Manufacture, Ministry of Education, School of Mechanical Engineering, Shandong University, Jinan 250061, China

[2] School of Mechanical and Manufacturing Engineering, The University of New South Wales (UNSW), Sydney, NSW, Australia

[3] School of Mechanical Engineering, Shenyang Jianzhu University, Shenyang 110168, China

[a]sdu_zzz@163.com, [b]retjli8366@163.com, [c]yaopeng@sdu.edu.cn, [d]jun.wang@unsw.edu.au, [e]chuanzhenh@sdu.edu.cn, [f]Zhangke@sjzu.edu.cn, [g]liuyue@sdu.edu.cn

Keywords: RB-SiC, Abrasive waterjet dressing, Diamond wheel, Orthogonal experiment

Abstract. To realize the high efficiency and precision machining of reaction sintered silicon carbide (RB-SiC). An on-machine abrasive waterjet method is proposed for dressing a metal-bonded diamond grinding wheel in this paper. These wheels were used for grinding RB-SiC. The grinding force and surface roughness were measured during the grinding process. The influence of grinding process parameters on the surface grinding force and surface roughness of the workpiece were analyzed by orthogonal experiments. This study provides an applicable method for controlling the surface quality of precision ground RB-SiC with the metal bonded diamond grinding wheel.

Introduction

High precision, ultra-smooth and lightweight primary mirror is the key to a new generation of space camera and other large high resolution optical remote sensing system[1]. Reaction sintered silicon carbide is expected to be one of the most excellent materials for space optics due to their many superior properties, such as high stiffness, high thermal conductivity, high wear resistance, and low thermal expansion coefficient. However, as a typical hard and brittle materials, reaction-bonded silicon carbide (RB-SiC) is difficult to achieve a high efficiency and low damage ultra-precision machining, which limits their further application in optical fields[2,3].

Precision grinding with a diamond wheel is regarded as one of the most appropriate methods to machine these hard and brittle materials[4], which is often used to reduce the shape errors rapidly in rough machining of a large-aperture aspheric mirror. However, the resinoid bonded diamond wheel wear is inevitable and fast during the machining process, which not only affect the surface roughness but also the form accuracy of the workpiece. Compared with resin bonded diamond grinding wheel, metal bonded diamond grinding wheel is easier to ensure the machining accuracy due to its higher strength, hardness, and lower wear rate. However, the form accuracy, surface and subsurface quality of the mirror will degrade seriously if the metal bonded grinding wheel is not timely dressed because of its poor self-sharpening [5]. Moreover, it is difficult to dress the metal bonded grinding wheel with the traditional mechanical dressing

method. Potential problems still need to be solved in conventional dressing, such as wear of the dressing tool and low dressing efficiency[6].

To address these problems, the abrasive waterjet technology was performed for dressing the wheel. Compared with conventional dressing methods, abrasive waterjet dressing neither causes mechanical damage on grains nor does it leads to a thermal effect on the grinding wheel. Thus, it is a promising tool for dressing of the wheel by abrasive waterjet[7]. Many efforts have been made by previous researchers in abrasive waterjet dressing. Hirao et al. [8] offered a proposal of using high-pressure waterjet to remove chips from the metal bonded CBN wheel without damaging the wheel. Axinte et al. [9] reported on a specific application of AWJ turning, i.e. truing and dressing of Al_2O_3 grinding wheels. The results of the experiment demonstrated that abrasive waterjet turning integrates the kinematics of a conventional turning process with the advantages of abrasive waterjet cutting. It will remove abrasive grits as well as binder on the circumference of the grinding wheel progressively. The results also showed that the accuracy of the trued wheel profile decreases as the stand-off distance increasing. Yao et al. [10] investigated the effect of AWJ dressing of resinoid bonded diamond wheels and concluded that the dressing effect of abrasive waterjet is superior to pure waterjet. The protrusion height of the diamond grits becomes distinct and the abrasive grains distribute uniformly on the wheel surface after dressing with abrasive waterjet. Although the abrasive waterjet dressing has been widely investigated, a limited number of studies which focused on the on-machine dressing metal bonded diamond wheel during grinding of RB-SiC have been reported.

In this study, the abrasive waterjet technology for dressing the metal bonded grinding wheel is introduced. The wheel surface topography before and after abrasive water jet dressing was compared and analyzed. In order to find the influence of the grinding parameters such as wheel speed, cutting depth, crossfeed rate and axial feed on the surface roughness and grinding force, the experiments of grinding of RB-SiC using the AWJ dressed diamond wheel were conducted by an orthogonal test method.

Experimental setup and Procedure

The experiments were conducted on an ultra-precision surface grinding machine NAS520 CNC. In these experiments, an on-machine dressing process termed abrasive waterjet dressing was used. The dressing process is illustrated in Fig. 1, and the detail dressing parameters are listed in Table 1. The metal bonded wheel size is about 200 mm in diameter and 8 mm in depth. The average grit size is 120 mesh. The topographies of wheel surface before and after dressing were observed by a 3D laser scanning confocal microscope (Keyence VK-X200K).

The RB-SiC ceramics employed in the experiments is fabricated by Changchun Institute of Optics, Fine Mechanics and Physics, CAS. The material properties of the samples are shown in Table 2. The workpiece was clamped on the three-component force dynamometer and fixed on the table of the surface grinder. The average surface roughness (Ra) of the workpiece was measured at five different positions on the surface by a portable surface roughness tester. The measuring direction is vertical to the feed direction of the table.

In order to find the influence of the grinding parameters (including wheel speed, cutting depth, cross feed rate and axial feed) on the surface roughness and grinding force, the grinding experiments were conducted in this paper by an orthogonal test method. The orthogonal test method is a kind of designing method to study many factors and levels. It conducts tests by selecting a suitable number of representative test cases from many test data, which have evenly dispersed, neat comparable characteristics. The design of orthogonal experimental is based on the orthogonal table. Table 3 lists the factors and levels of the orthogonal experiment in which

four grinding parameters including (A) wheel speed (B) cutting depth, (C) feed rate, and (D) axial feed were selected. Each parameter has five levels to be optimized. Twenty-five trials were carried out according to the L_{25} (5^6) array to grinding RB-SiC to complete the optimization process.

Table 1 The detail dressing parameters

Orifice diameter (mm)	0.25
Nozzle diameter (mm)	0.76
Abrasive in waterjet	150# (75 to 106 μm)
Jet pressure(MPa)	40
Standoff distance(mm)	20
Wheel speed(m/s)	5

Table 2 Physical and mechanical properties of RB-SiC ceramics

Property	Values
Density (g/cm^3)	3.0
Young modulus (GPa)	350
Poisson's ratio υ	0.24
Thermal conductivity (W/m×k)	144[11]
Thermal expansion coefficient ($K^{-1}\times10^{-6}$)	2.4

Table 3 The factors and levels of the orthogonal experiment

Level	Factor			
	Wheel speed v_s (A) (m/s)	Cutting depth a_p (B) (μm)	Feed rate v_w(C) (mm/min)	Axial feed f_a (D) (mm)
1	10	2	6800	2
2	15	4	10200	2.5
3	20	6	13600	3
4	25	8	17000	3.5
5	30	10	20400	4

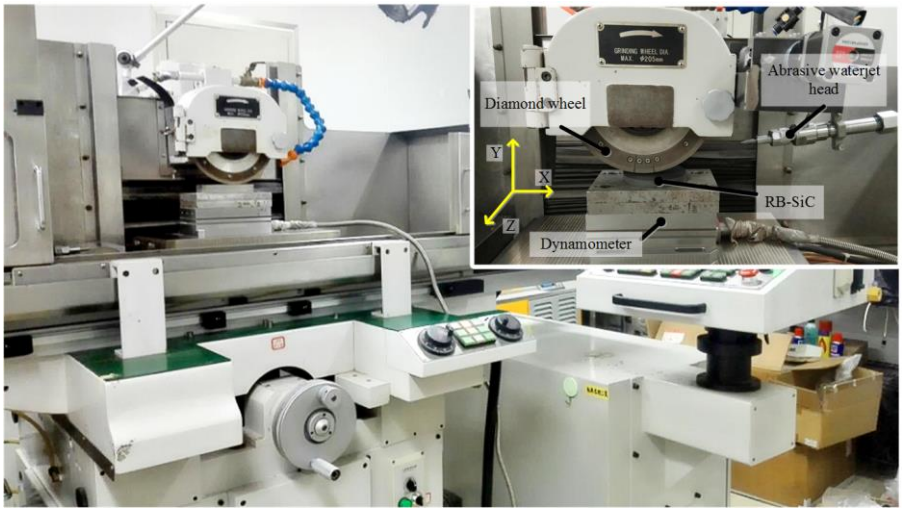

Fig. 1 Experiment setup for dressing of wheel and grinding of RB-SiC

Results and discussion

Wheel surface topography before and after dressing. Fig. 2 shows the wheel surface topography of diamond grinding wheel after grinding RB-SiC ceramic, the wheel wear involved diamond grits flattening and dislodgement. The flattening of the diamond grits increases the frictional effects and thermal loading due to the decreasing number of cutting edges involved in material removal. Therefore, graphitization of the diamond grits could be caused by the high pressure and temperature during the interaction process of diamond grits and workpiece, which affects grinding performance. When compared with the original grain surface, the diamond grains after abrasive waterjet dressing shown in Fig. 2 (b) display good dressing quality with high protrusion height, indicating the feasibility of using the abrasive waterjet to sharpen metal bonded diamond wheel. Moreover, many angular diamond abrasives stick out of the wheel surface, which is because the removal rate of the binder is higher than that of the diamond grits while abrasive waterjet impacting on the surface of the grinding wheel. As shown in Fig. 3. The runout of the diamond grinding wheel after grinding RB-SiC ceramic and after dressing are 2.9 μm and 3.9 μm, respectively. The results proved that not only does this may cause the good dressing quality, and not affect too greatly to the variation of the wheel radial runout.

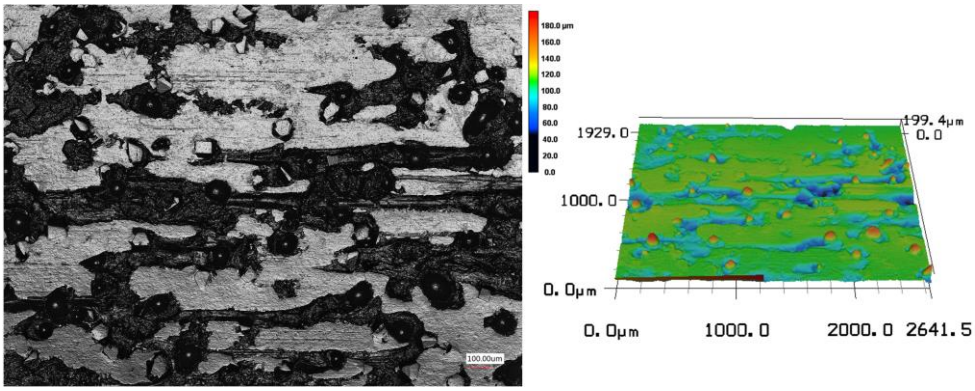

(a) Wheel surface before dressing（200×）

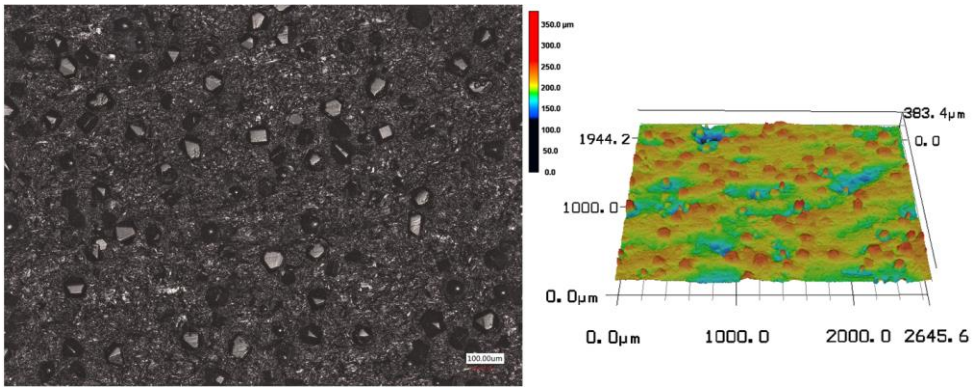

(b) Wheel surface after dressing（200×）

Fig. 2 Comparison of surface topographies of wheel before and after dressing

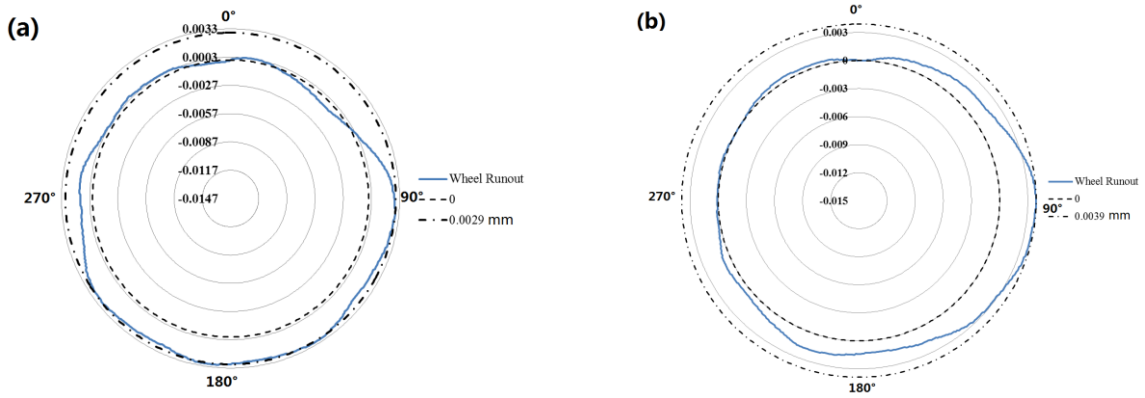

(a)Wheel runout before dressing (b)Wheel runout after dressing

Fig. 3 Radar maps of runout of grinding wheel before and after dressing

Grinding force and surface roughness in grinding of RB-SiC. The sorted ranges of the orthogonal results are shown in Table 4, on the basis of the data and Range R results, the influence of four factors on grinding force can be ranked as follows: A > B > C > D. Therefore, the difference in wheel speed influenced grinding force the most, followed by the cutting depth, feed rate, and axial feed. The optimum combination is selected as $A_5B_1C_5D_4$. The optimum parameters by orthogonal experiment optimum design are v_s = 30 m/s, a_p = 2 μm, v_w = 20400 mm/min and f_a=3.5 mm. In addition, it can be found that the influence of grinding parameters on the surface roughness Ra values: the effect of wheel speed is the most significant, the second important factor is the feed rate, and the effect of the cutting depth is the least. The optimum combination is selected as $A_1B_1C_1D_1$. The optimum parameters by orthogonal experiment optimum design are v_s = 10 m/s, a_p = 2 μm, v_w = 6800 mm/min and f_a=2 mm. The surface topography of the ground SiC which have minimum and maximum roughness were shown in Fig. 4(a) and (b), respectively. The surface topography of the ground SiC Ⅷ appears even worse than that of the ground SiC Ⅰ, a multitude of micro cracks are distributed on the surface. The results showed that there is more brittle removal in the ground SiC Ⅷ.

Table 4 Range analysis of the grinding force and the surface roughness

Trial No.	Wheel speed v_s (A) (m/s)	Cutting depth a_p (B) (μm)	Feed rate v_w(C) (mm/min)	Axial feed f_a (D) (mm)	Maximum undeformed chip thickness （μm）	Grinding force（N)	Surfaces roughness（μm）
1	10	2	6800	2	0.230	87.6	0.195
2	10	4	10200	2.5	0.487	148	0.32
3	10	6	13600	3	0.796	188	0.33
4	10	8	17000	3.5	1.149	204.8	0.42
5	10	10	20400	4	1.541	218	0.42
6	15	2	10200	3	0.230	56.55	0.3
7	15	4	13600	3.5	0.433	118.3	0.41

8	15	6	17000	4	0.663	164.8	0.43
9	15	8	20400	2	0.919	131.3	0.34
10	15	10	6800	2.5	0.343	97.85	0.31
11	20	2	13600	4	0.230	64.65	0.33
12	20	4	17000	2	0.406	73.87	0.23
13	20	6	20400	2.5	0.597	109.7	0.37
14	20	8	6800	3	0.230	77.8	0.28
15	20	10	10200	3.5	0.385	125.7	0.35
16	25	2	17000	2.5	0.230	49.84	0.25
17	25	4	20400	3	0.390	82.67	0.29
18	25	6	6800	3.5	0.159	66.91	0.25
19	25	8	10200	4	0.276	113.8	0.3
20	25	10	13600	2	0.411	96	0.27
21	30	2	20400	3.5	0.230	47.17	0.3
22	30	4	6800	4	0.108	53.4	0.2
23	30	6	10200	2	0.199	55.15	0.24
24	30	8	13400	2.5	0.302	98.29	0.26
25	30	10	17000	3	0.428	128.47	0.25
Range R_1	92.78	72.04	47.64	34.15			
Order of the factor(grinding force)	A→B→C→D						
Range R_2	0.108	0.049	0.097	0.091			
Order of the factor(surfaces roughness)	A→C→D→B						

Fig. 5 shows the effects of grinding parameters on the grinding force of orthogonal experiment products. Specifically, Fig. 5(a) illustrates that an increase in wheel speed reduces grinding force. As a result of the number of abrasive grains in the grinding area increasing as the speed of the grinding wheel increasing, the load of single grain decreases. According to Fig. 5(b) and (c), the grinding force exhibited a trend of significant increase with the increase in cutting depth and workpiece feed rate. This finding may be attributed to the fact that the increased undeformed chip thickness improved the load of single grain. The grinding force affected by different axial feed was seen in Fig. 5(d), the grinding force increased with an increase in axial feed. This phenomenon may be due to increasing of the number of abrasive grits involved in grinding.

Fig. 6 shows the effects of grinding parameters on the surface roughness of orthogonal experiment products. According to Fig. 6(a)-(c), the surface roughness exhibited a trend of

significant decrease with wheel speed increase, whereas that of surface roughness decreased with the increase in cutting depth and workpiece feed rate. This process may be induced by the change of the undeformed chip. A decrease in the undeformed chip will decrease surface roughness, which in turn, produces an increase in the surface damage and roughness. Fig. 6(d) illustrates that the relation of the axial feed to surface roughness is directly attributed to a large increase in grinding forces that accompany an increase in axial feed. Eventually leads to an increase in the surface region plastics, surface damage and high average surface roughness.

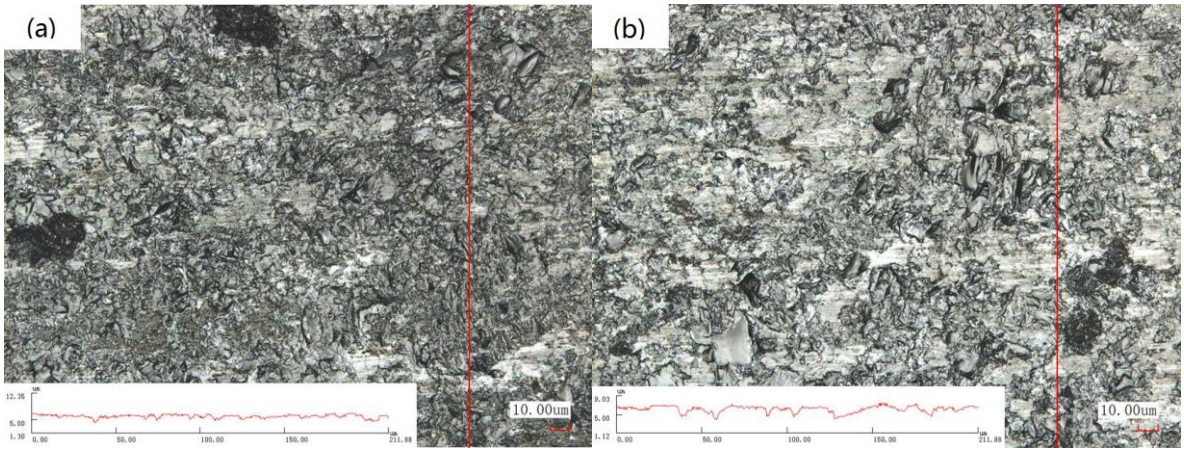

(a) Surface topography of the ground RB-SiC Ⅰ (b) Surface topography of the ground RB-SiC Ⅷ

Fig. 4 Surface topography of the ground RB-SiC

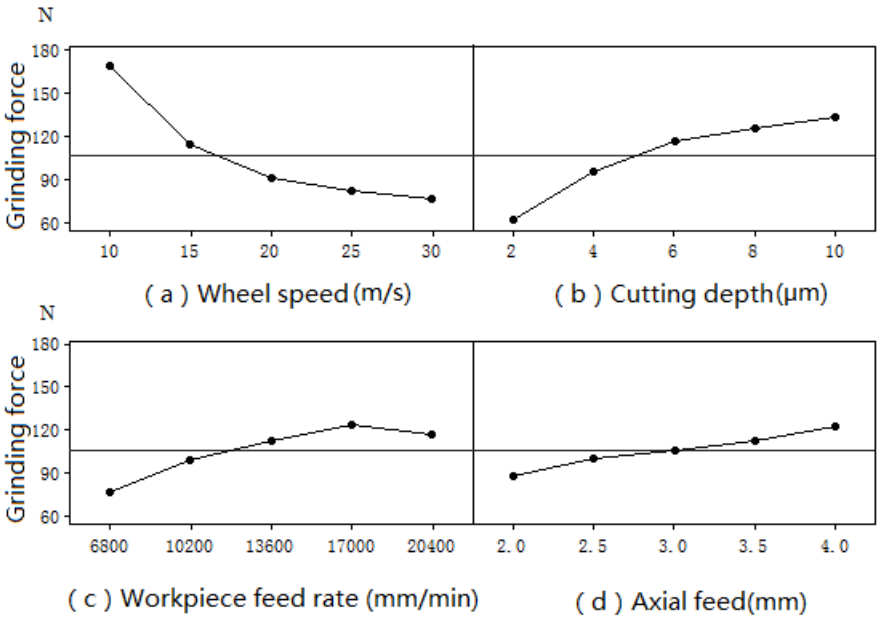

Fig. 5 The effects of grinding parameters on grinding force

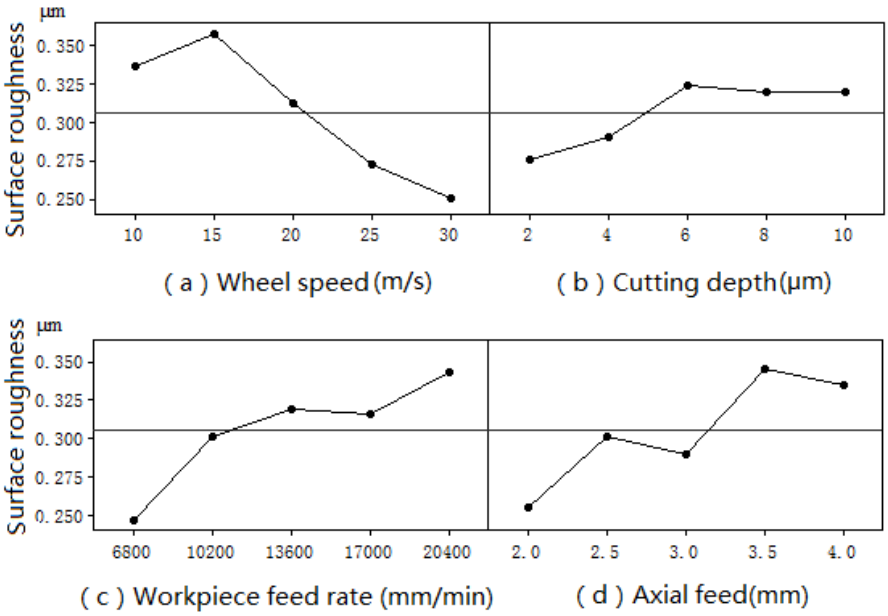

Fig. 6 The effects of grinding parameters on surface roughness

Conclusion

This study presented the use of abrasive waterjet method for dressing a metal bond diamond wheel for precision grinding of RB-SiC ceramics. The wheel surface topographies before and after abrasive water jet dressing were compared and analyzed. The results showed the grains on the surface of the grinding wheels protruded well from binder after AWJ dressing. The surface grinding of RB-SiC experiments designed by the orthogonal test method were carried out with abrasive waterjet dressed grinding wheel. The wheel speed has the greatest influence on the grinding force and surface roughness. The optimum combination of parameters are selected as $A_5B_1C_5D_4$ for grinding force, $A_1B_1C_1D_1$ for surface roughness.The optimum parameters by orthogonal experiment optimum design are v_s = 30 m/s, a_p = 2 μm, v_w = 20400 mm/min and f_a=3.5 mm for grinding force, v_s = 10 m/s, a_p = 2 μm, v_w = 6800 mm/min and f_a=2 mm for surface roughness.

Acknowledge

This project was funded by Key Laboratory of Optical System Advanced Manufacturing Technology (Grant No. Y4GX1SJ141 and Y6SY1FJ160-01), Shandong Natural Science Foundation (Grant No. ZR2018MEE019).

References

[1] G Zhang, W Zhao, R Zhao, J Bao, B Dong, C Cui, X Wang, Q Cao: Fabricating large-scale mirrors using reaction-bonded silicon carbide. SPIE Newsroom (2016).

[2] Z Dong, H Cheng: Ductile mode grinding of reaction-bonded silicon carbide mirrors. Applied Optics 56 (2017).

[3] H Liang, X Yao, H Zhang, X Liu, Z Huang: Friction and wear behavior of pressureless liquid phase sintered SiC ceramic. Materials & Design 65 (2015) 370-76.

[4] E Brinksmeier, Y Mutlugünes, F Klocke, JC Aurich, P Shore, H Ohmori: Ultra-precision grinding. CIRP Annals-Manufacturing Technology 59 (2010) 652-71.

[5] P V Witzendorff, M Stompe, A Moalem: Dicing of hard and brittle materials with on-machine laser-dressed metal-bonded diamond blades. Precision Engineering, 38(2014):162-167.

[6] Q Zhang, Q Zhao, S To, B Guo, W Zhai: Diamond wheel wear mechanism and its impact on the surface generation in parallel diamond grinding of RB-SiC/Si. Diamond & Related Materials 74 (2017) 16-23.

[7] Z Zhang, P Yao, Z Zhang, D Xue, C Wang, C Huang, H Zhu: A novel technique for dressing metal-bonded diamond grinding wheel with abrasive waterjet and touch truing. The International Journal of Advanced Manufacturing Technology 93 (2017) 3063-73.

[8] M Hirao, M Izawa, N Iguchi, K Shirase, T Yasui: Waterjet In-process Dressing (1st Report). Journal of the Japan Society for Precision Engineering 64 (1998) 1335-39.

[9] DA Axinte, JP Stepanian, MC Kong, J McGourlay: Abrasive waterjet turning—An efficient method to profile and dress grinding wheels. International Journal of Machine Tools and Manufacture 49 (2009) 351-56.

[10] P Yao, W Wei, CZ Huang, J Wang, HT Zhu, ZY Zhang: High Efficiency Abrasive Waterjet Dressing of Diamond Grinding Wheel. Advanced Materials Research 1017 (2014) 243-48.

[11] X Rao, F Zhang, C Li, Y Li: Experimental investigation on electrical discharge diamond grinding of RB-SiC ceramics. International Journal of Advanced Manufacturing Technology (2017) 1-12.